Supplementary Figures For Publication

Full Title:

Functional characterization of the human Dicer1e isoform reveals non-canonical RNA processing and context-dependent remodeling of cellular regulatory networks

Short Running Title:

Beyond miRNA biogenesis: Dicer1e as a non-canonical regulator of cell metabolism

Marta Wojnicka, Arkadiusz Kajdasz, Lukasz Marczak, Piotr H. Malecki, Aleksander Strugala, Klaudia Wojcik, Konrad Kuczynski, Anna Philips, Anna Kurzynska-Kokorniak*

Institute of Bioorganic Chemistry, Polish Academy of Sciences, 61-704 Poznan, Poland

***corresponding author: akurzyns@man.poznan.pl**

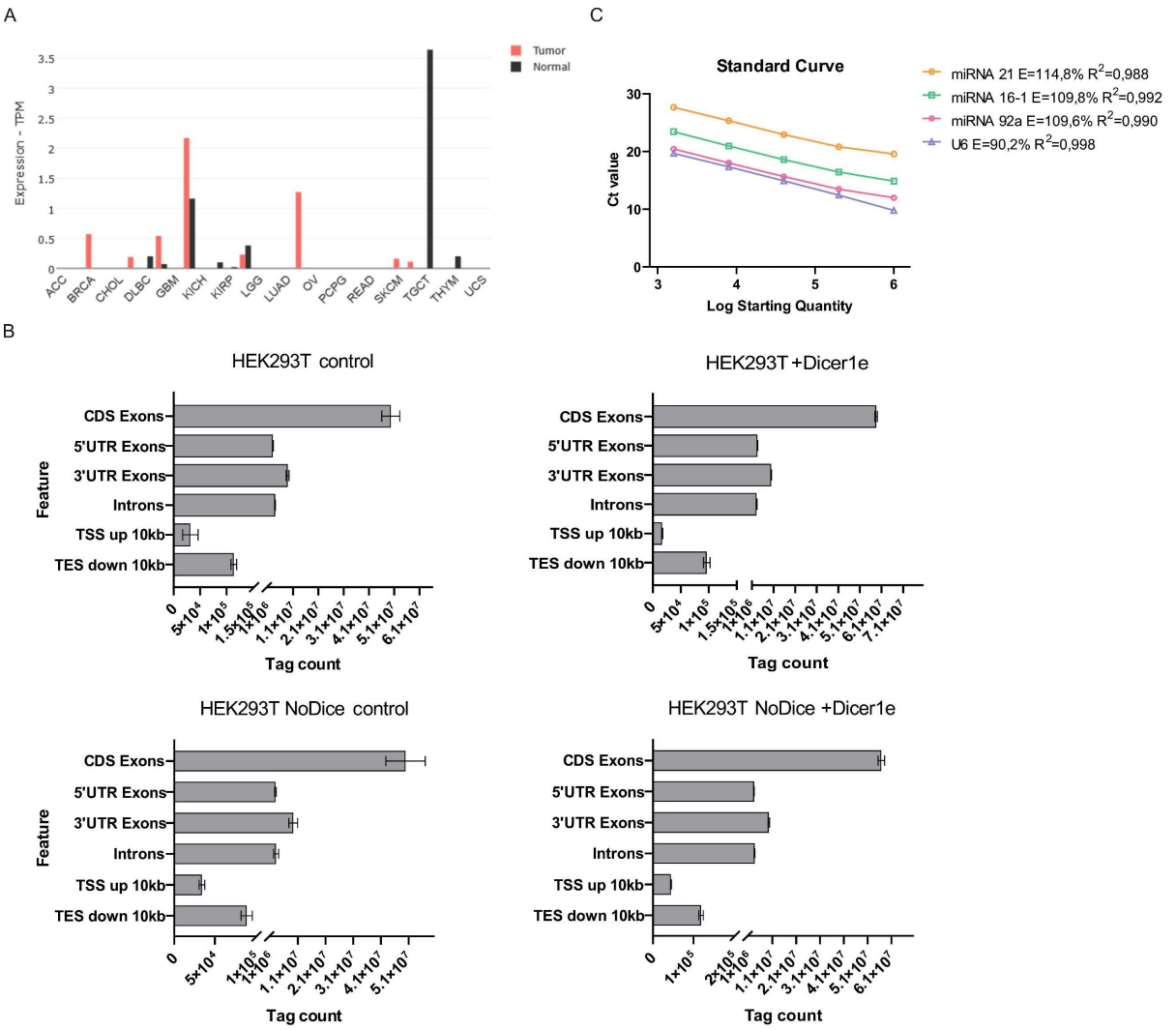

Supplementary Figure S1

Supporting analyses related to Dicer1e expression profiling, RNA-Seq data quality, and qPCR validation. (A) Expression of the Dicer1e transcript across human tumor and paired normal tissues based on GEPIA2 analysis of TCGA and GTEx datasets. Bar heights represent median expression levels for individual tumor types and corresponding normal tissues. ACC, adrenocortical carcinoma; BRCA, breast invasive carcinoma; CHOL, cholangiocarcinoma; DLBC, diffuse large B-cell lymphoma; GBM, glioblastoma multiforme; KICH, kidney chromophobe; KIRP, kidney renal papillary cell carcinoma; LGG, lower grade glioma; LUAD, lung adenocarcinoma; OV, ovarian serous cystadenocarcinoma; PCPG, pheochromocytoma and paraganglioma; READ, rectum adenocarcinoma; SKCM, skin cutaneous melanoma;

TGCT, testicular germ cell tumors; THYM, thymoma; UCS, uterine carcinosarcoma. **(B)** Distribution of RNA-Seq reads across genomic features. Average read counts from three biological replicates (n = 3) are shown for control cells (left panels) and cells transfected with the Flag-tagged Dicer1e expression vector (right panels). TSS up 10 kb, region 10 kb upstream of the transcription start site; TES up 10 kb, region 10 kb downstream of the transcription end site. **(C)** Standard curves used to determine qPCR primer efficiencies for miR-21, miR-16, miR-92a, and U6. Curves were generated using five-fold serial dilutions of cDNA template (40, 8, 1.6, 0.32, and 0.064 ng per reaction). Amplification efficiencies (E) and coefficients of determination (R^2) are indicated for each primer pair.

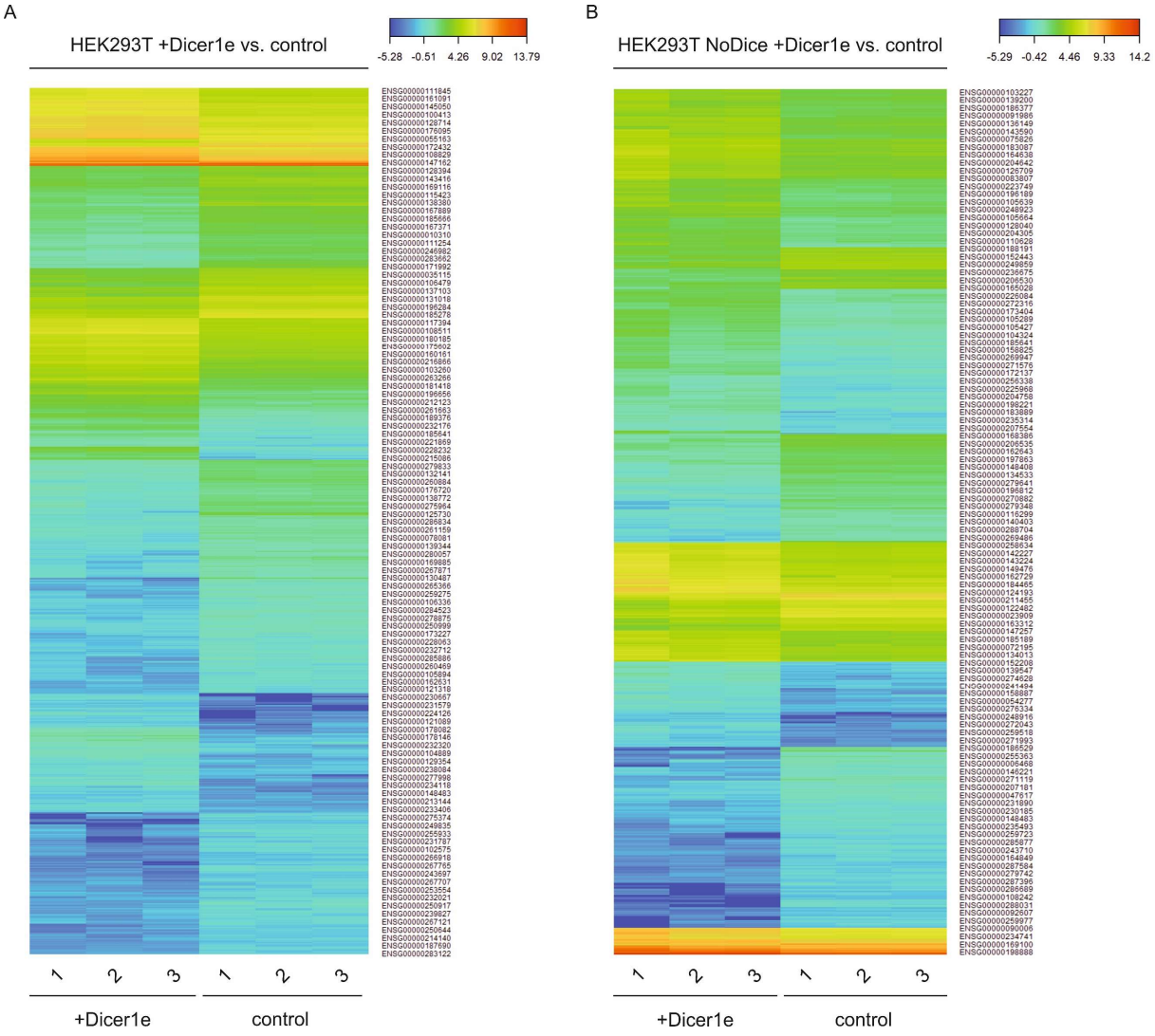

Supplementary Figure S2

Heat maps showing differential gene expression following Dicer1e expression. (A) Heat map of differentially expressed genes (DEGs) in HEK293T cells comparing Dicer1e-expressing cells with control cells. **(B)** Heat map of DEGs in HEK293T NoDice cells, comparing Dicer1e-expressing cells with control cells. DEGs were defined as genes with FDR < 0.05 and $|\log_2 FC| > 1$. Red and blue indicate relatively higher and lower gene expression levels, respectively.

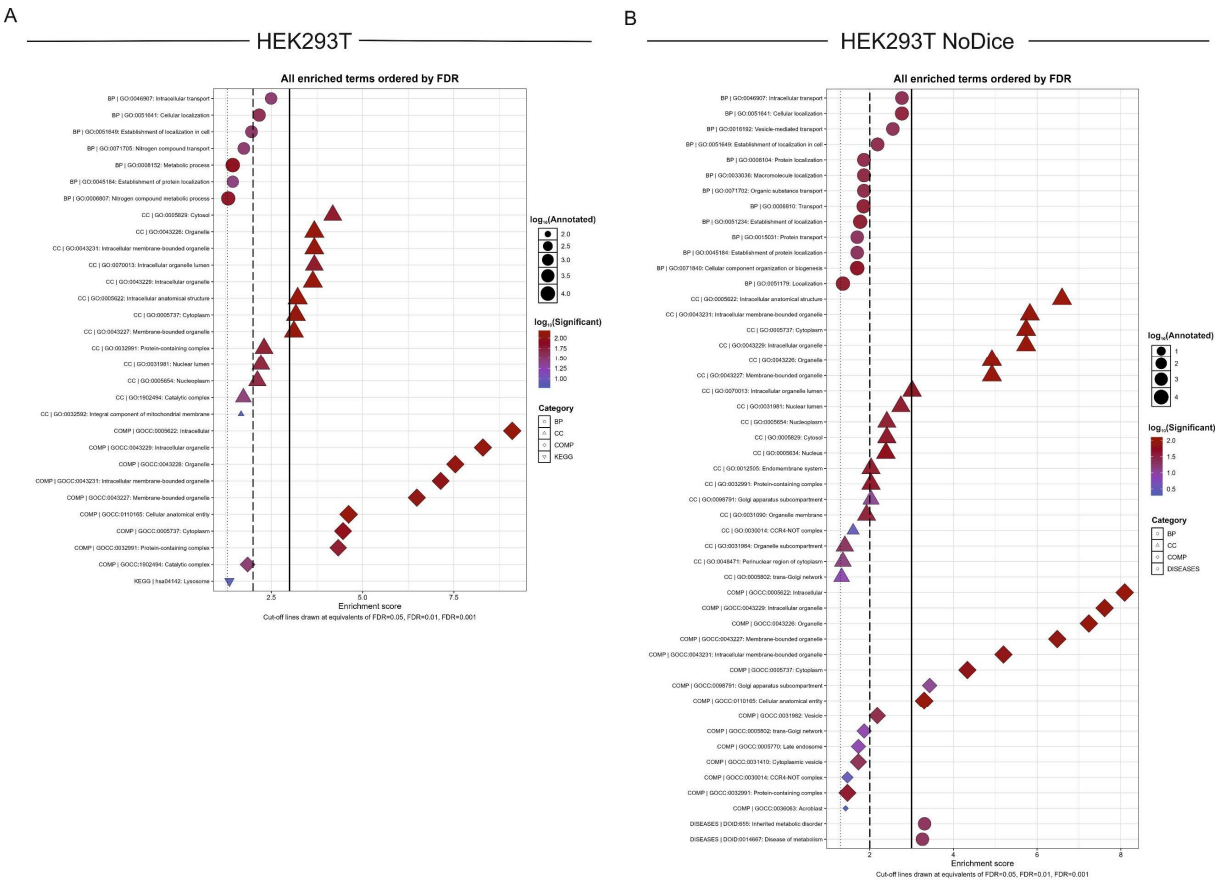

Supplementary Figure S3

Summary of functional enrichment analysis of differentially abundant proteins upon Dicer1e expression. (A) and **(B)** show enriched functional terms identified among differentially abundant proteins (DAPs) in HEK293T and HEK293T NoDice cells expressing the Dicer1e variant, respectively. The most significantly enriched Biological Process (BP), Cellular Component (CC), and Compartment (COMP) terms are ordered according to the false discovery rate (FDR). The x-axis represents the enrichment score, point color indicates statistical significance ($-\log_{10}$ adjusted p value), and point size reflects the number of proteins annotated to each term. Functional enrichment analysis was performed using STRING on DAPs identified with $p < 0.05$ and $|\log_2 FC| \geq 1$.

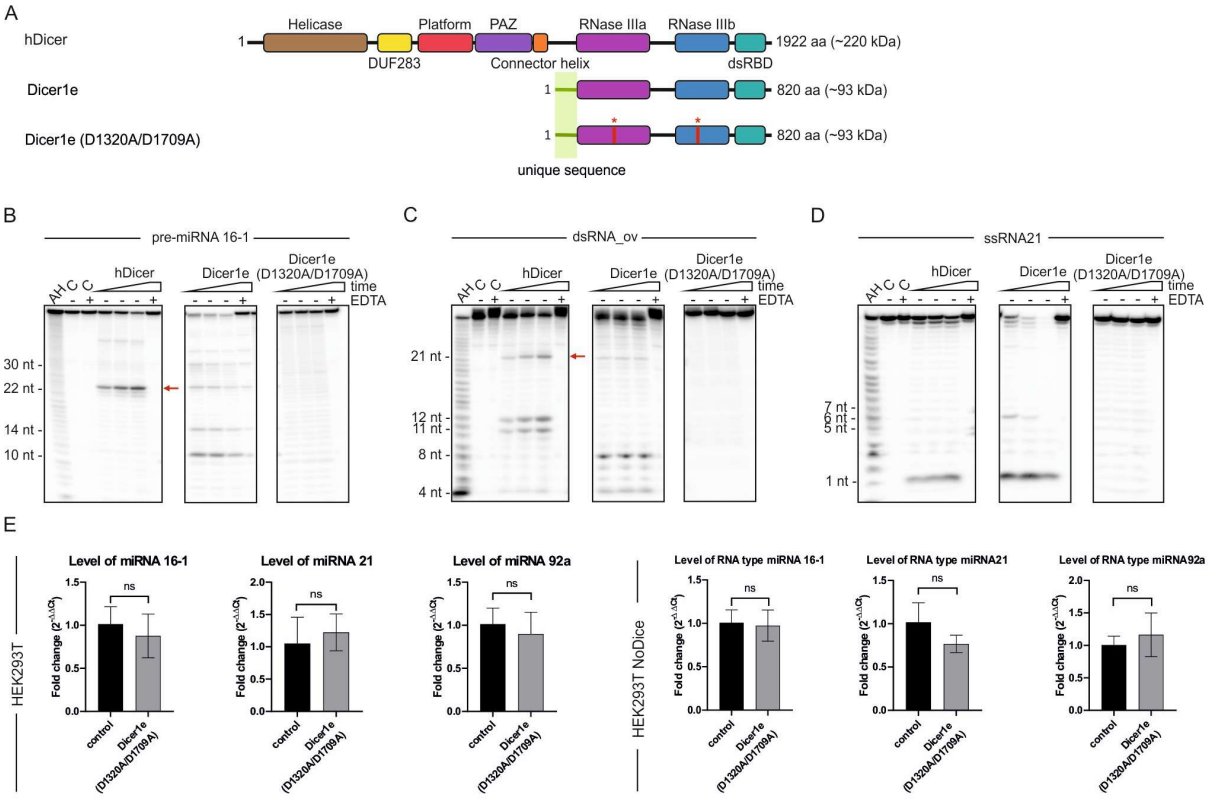

Supplementary Figure S4

RNase activity of Dicer1e and its catalytic mutant. (A) Schematic representation of the domain architecture of full-length hDicer, Dicer1e, and the catalytically inactive Dicer1e mutant (D1320A/D1709A). The unique 13-amino-acid N-terminal sequence of Dicer1e is highlighted in green. **(B–D)** Time-dependent RNA cleavage assays performed with **(B)** pre-miR-16-1, **(C)** a 30-bp dsRNA substrate containing 2-nt 3′ overhangs, and **(D)** a 21-nt miRNA mimic (ssRNA21). Triangles indicate incubation times of 15, 30, and 60 min. Reactions were performed using 12.5 nM recombinant protein. (*C-*) Control reactions lacking protein. (*C+EDTA*) Control reactions lacking protein and supplemented with 25 mM EDTA. (*+EDTA*) Reactions supplemented with 25 mM EDTA in the presence of recombinant protein. EDTA chelates Mg^{2+} ions required for RNase III activity and thereby inhibits RNA cleavage. (*AH*) Alkaline hydrolysis ladder generated from 5′-^{32}P-labeled RNA substrates. Red arrows indicate the canonical hDicer cleavage products. **(E)** Expression levels of selected miRNAs in

HEK293T and HEK293T NoDice cells 48 h after transfection with a FLAG-tagged catalytically inactive Dicer1e mutant (D1320A/D1709A). miRNA levels were normalized to U6 snRNA and expressed relative to cells treated with transfection reagent alone (control). Data are presented as mean ± SD from three biological replicates (n = 3). Statistical significance was assessed using an unpaired two-tailed Student's *t*-test.

A

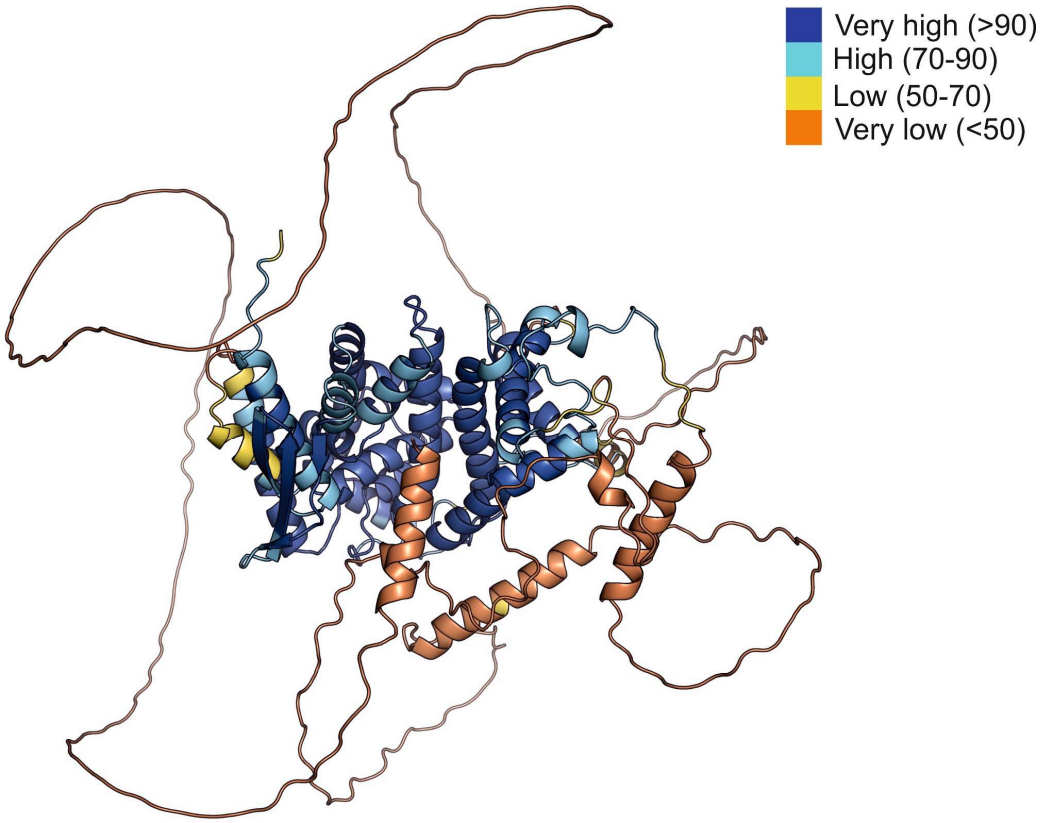
Very high (>90)
High (70-90)
Low (50-70)
Very low (<50)

B

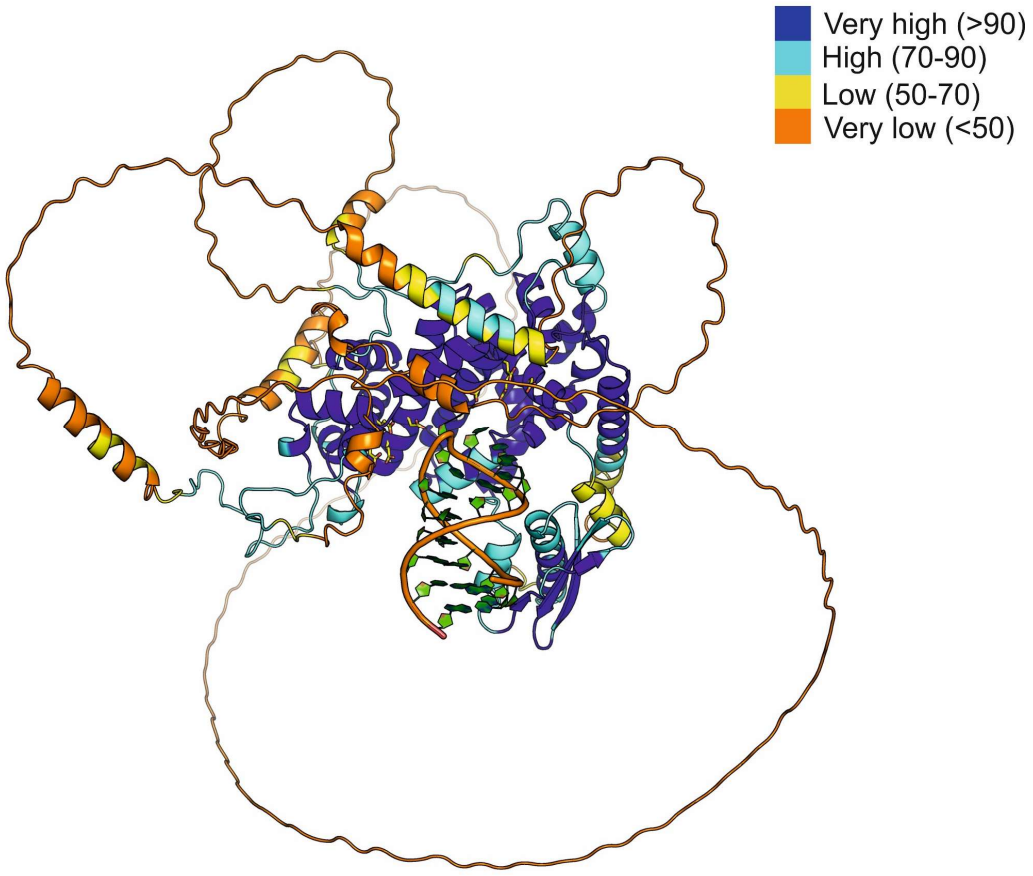
Very high (>90)
High (70-90)
Low (50-70)
Very low (<50)

Supplementary Figure S5

Per-residue local distance difference test (pLDDT) confidence scores mapped onto AlphaFold3 models of Dicer1e. (A) Dicer1e. The color scale indicates model confidence as shown in the legend. The catalytic core comprising the RNase IIIa and RNase IIIb domains, together with the dsRBD domain, is predicted with high confidence, whereas the N-terminal extension and extended loop regions display lower confidence scores. **(B)** Dicer1e modeled in complex with a 21-nt RNA substrate. Confidence scores are shown using the same color scale as in panel A. High-confidence predictions are concentrated within the structured catalytic core, whereas lower-confidence regions correspond predominantly to peripheral flexible loops and terminal segments.